A Minimum-Complexity Failure Correction Technique for Linear Arrays

F. Zardi, G. Oliveri, M. Salucci, and A. Massa

Contents

1 Numerical Results - Non-Iterative MCFC

1.1 Test case 5—Dolph-Chebyshev, $N \in \{50, 100, 150, 200\}$, SLL$=-25$ [dB], 4% faulty elements

1.1.1 Goal of the analysis

The goal of test case 5 is that of understanding the behavior of the MFC method developed for increasing array sizes. To that end, four arrays of different size will be considered, each with 4% faulty elements in the same positions.

1.1.2 Parameters

Array with 50 elements

The array considered has the following properties

- Number of array elements: $N = 50$
- Tapering: Dolph-Chebyshev, SLL$=-25$ [dB]
- Damaged element indexes set: $\Omega = \{4, 10\}$
- Number of faulty elements: $D = 4\%\times$
- Damaged element excitation: $\mathbf{w}_{\text{corr,immut}} = [0, 0,]$

The parameters used to configure the software for the array with $N = 50$ elements are the following:

- Phase 1
  - Desired SLL: $\text{SLL}^{(1)} = -25.5$ [dB]
    - Mask main lobe width: $\text{BW}^{(1)} = 5.5$ [deg]
    - Mask u samples count: $K^{(1)} = 5000$
- Phase 2
  - Desired SLL: $\text{SLL}^{(1)} = -25$ [dB]
  - Mask main lobe width: $\text{BW}^{(1)} = 5.5$ [deg]
  - Mask u samples count: $K^{(1)} = 2000$
- Use Hessian: Yes

Figure 1 shows the original excitations and the damaged ones for array with $N = 50$ elements.

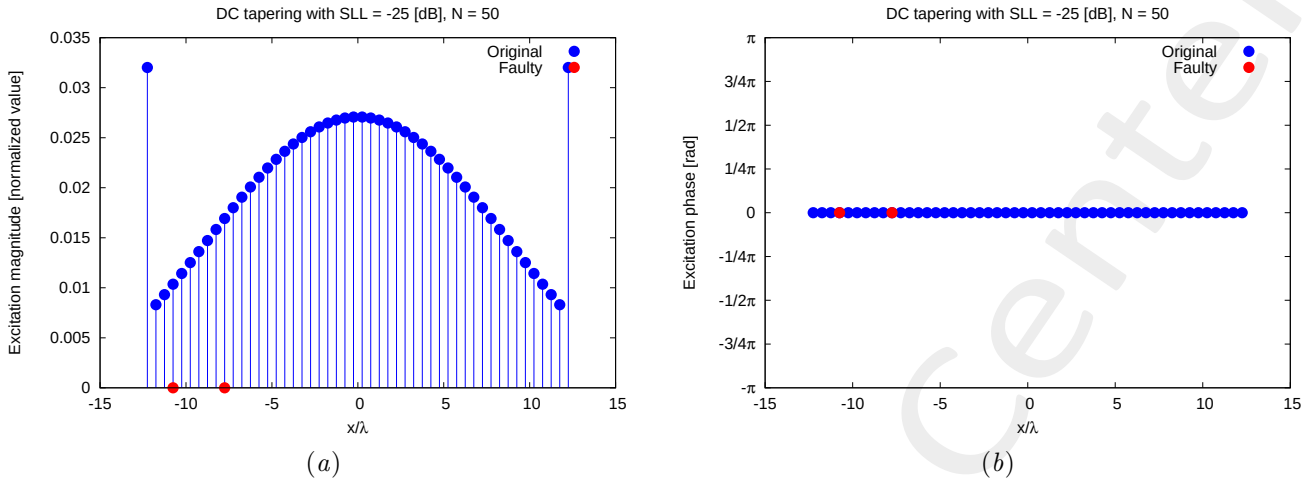

(a) (b)

Figure 1: Original and damaged excitations for the array with $N = 50$ elements considered in test case 5: amplitude (a) and phase (b).

Array with 100 elements

The arrays considered the following properties

- Number of array elements: $N = 100$
- Tapering: Dolph-Chebyshev, SLL$=-25$ [dB]
- Damaged element indexes set: $\Omega = \{8, 9, 20, 21\}$
- Number of faulty elements: $D = 4\% \times N$
- Damaged element excitation: $\mathbf{w}_{\text{corr,immut}} = [0, 0, 0, 0]$

The parameters used to configure the software for the array with $N = 100$ elements are the following:

- Phase 1
  - Desired SLL: $\text{SLL}^{(1)} = -25.5$ [dB]
    - Mask main lobe width: $\text{BW}^{(1)} = 2.8$ [deg]
    - Mask u samples count: $K^{(1)} = 1000$
- Phase 2
  - Desired SLL: $\text{SLL}^{(1)} = -25.0$ [dB]
  - Mask main lobe width: $\text{BW}^{(1)} = 2.8$ [deg]
  - Mask u samples count: $K^{(1)} = 1000$
- Use Hessian: Yes

Figure 2 shows the original excitations and the damaged ones for array with $N = 100$ elements.

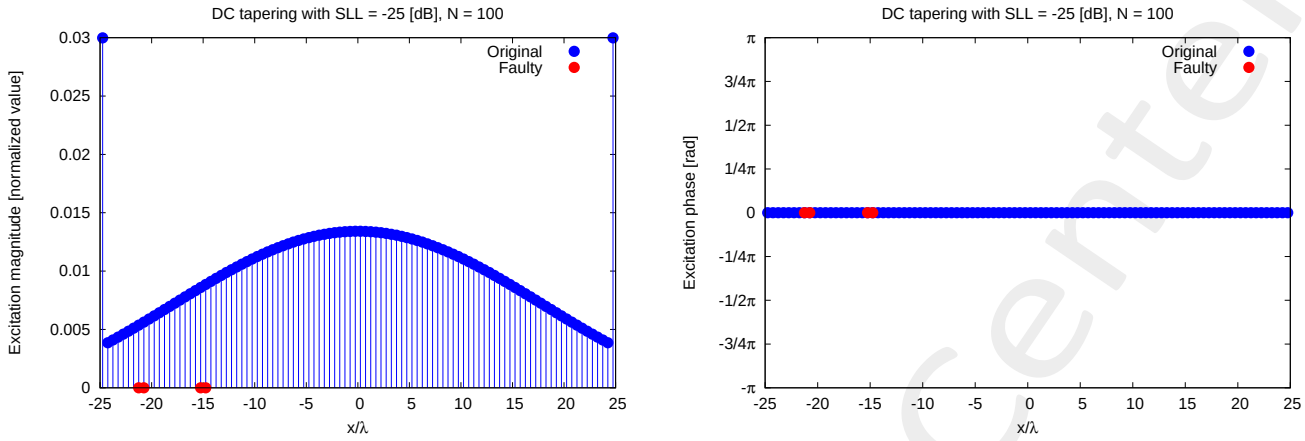

(a) (b)

Figure 2: Original and damaged excitations for the array with $N = 100$ elements considered in test case 5: amplitude (a) and phase (b).

Array with 150 elements

The arrays considered the following properties

- Number of array elements: $N = 150$
- Tapering: Dolph-Chebyshev, SLL$=-25$ [dB]
- Damaged element indexes set: $\Omega = \{12, 13, 14, 30, 31, 32\}$
- Number of faulty elements: $D = 4\% \times N$
- Damaged element excitation: $\mathbf{w}_{\text{corr,immut}} = [0, 0, 0, 0, 0, 0]$

The parameters used to configure the software for the array with $N = 150$ elements are the following:

- Phase 1
  - Desired SLL: $\text{SLL}^{(1)} = -25.5$ [dB]
    - Mask main lobe width: $\text{BW}^{(1)} = 1.8$ [deg]
    - Mask u samples count: $K^{(1)} = 1500$
- Phase 2
  - Desired SLL: $\text{SLL}^{(1)} = -25.0$ [dB]
  - Mask main lobe width: $\text{BW}^{(1)} = 1.8$ [deg]
  - Mask u samples count: $K^{(1)} = 1500$
- Use Hessian: Yes

Figure 3 shows the original excitations and the damaged ones for array with $N = 150$ elements.

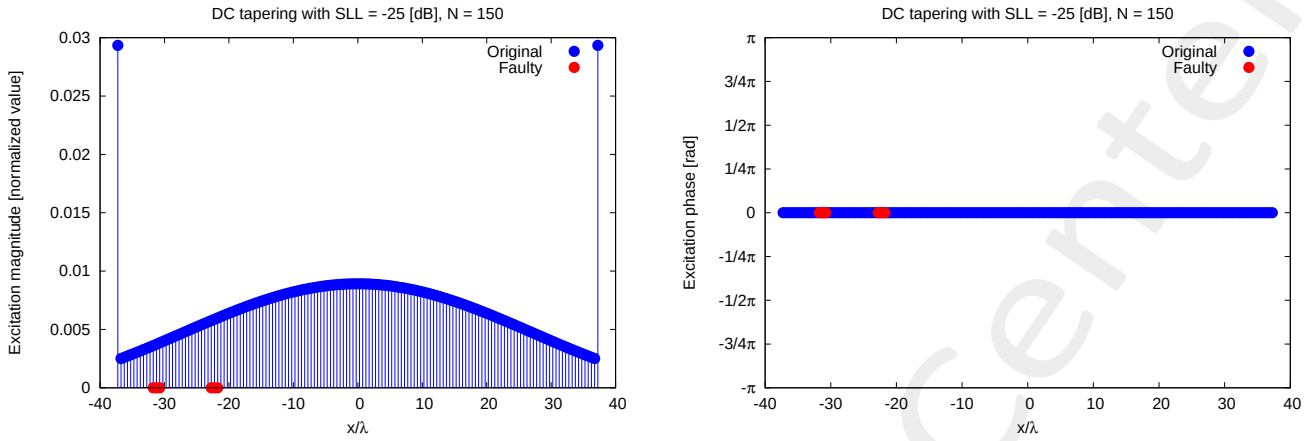

(a) (b)

Figure 3: Original and damaged excitations for the array with $N = 150$ elements considered in test case 5: amplitude (a) and phase (b).

Array with 200 elements

The arrays considered the following properties

- Number of array elements: $N = 200$
- Tapering: Dolph-Chebyshev, SLL$=-25$ [dB]
- Damaged element indexes set: $\Omega = \{16, 17, 18, 19, 40, 41, 42, 43\}$
- Number of faulty elements: $D = 4\% \times N$
- Damaged element excitation: $\mathbf{w}_{\text{corr,immut}} = [0, 0, 0, 0, 0, 0, 0, 0]$

The parameters used to configure the software for the array with $N = 200$ elements are the following:

- Phase 1
  - Desired SLL: $\text{SLL}^{(1)} = -25.5$ [dB]
    - Mask main lobe width: $\text{BW}^{(1)} = 1.4$ [deg]
    - Mask u samples count: $K^{(1)} = 2000$
- Phase 2
  - Desired SLL: $\text{SLL}^{(1)} = -25.0$ [dB]
  - Mask main lobe width: $\text{BW}^{(1)} = 1.4$ [deg]
  - Mask u samples count: $K^{(1)} = 2000$
- Use Hessian: Yes

Figure 4 shows the original excitations and the damaged ones for array with $N = 200$ elements.

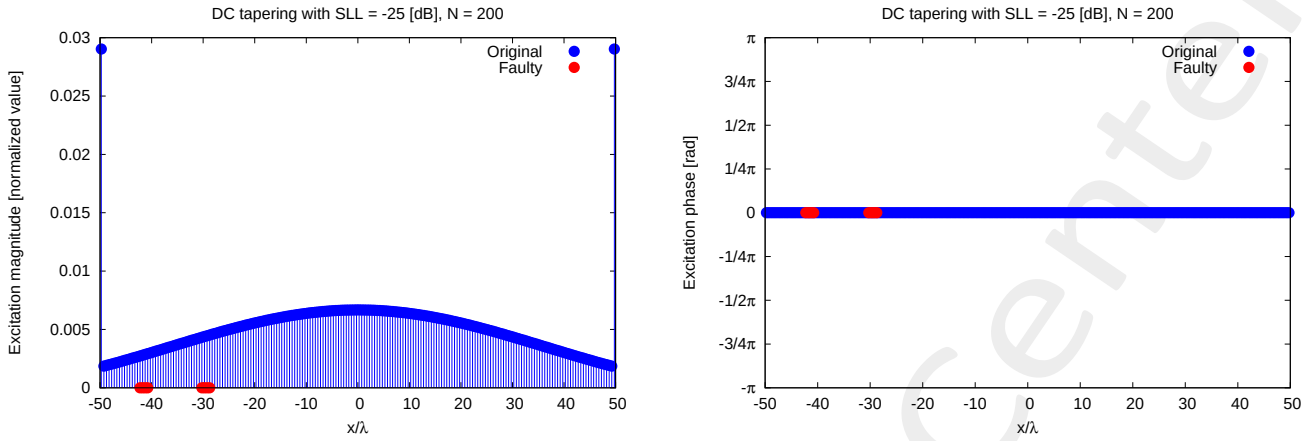

(a) (b)

Figure 4: Original and damaged excitations for the array with $N = 200$ elements considered in test case 5: amplitude (a) and phase (b).

1.1.3 Results

Array with 50 elements

Figure 5 compares the original excitations with the corrected excitations obtained with the proposed method for the array with 50 elements.

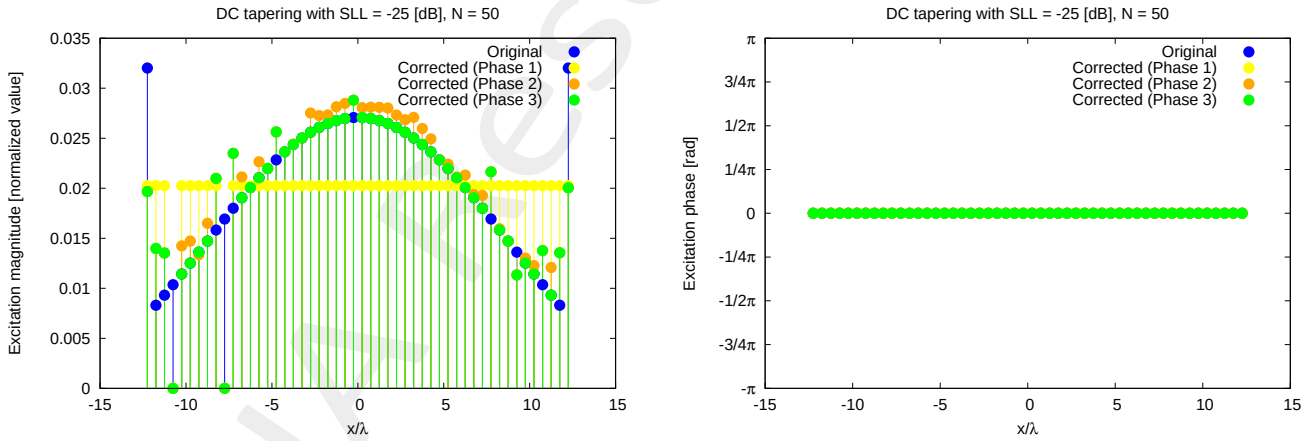

(a) (b)

Figure 5: Original and corrected excitations for the array with 50 elements: amplitude (a) and phase (b).

Figure 6 compares the original, faulty and corrected radiation patterns for the array with 50 elements.

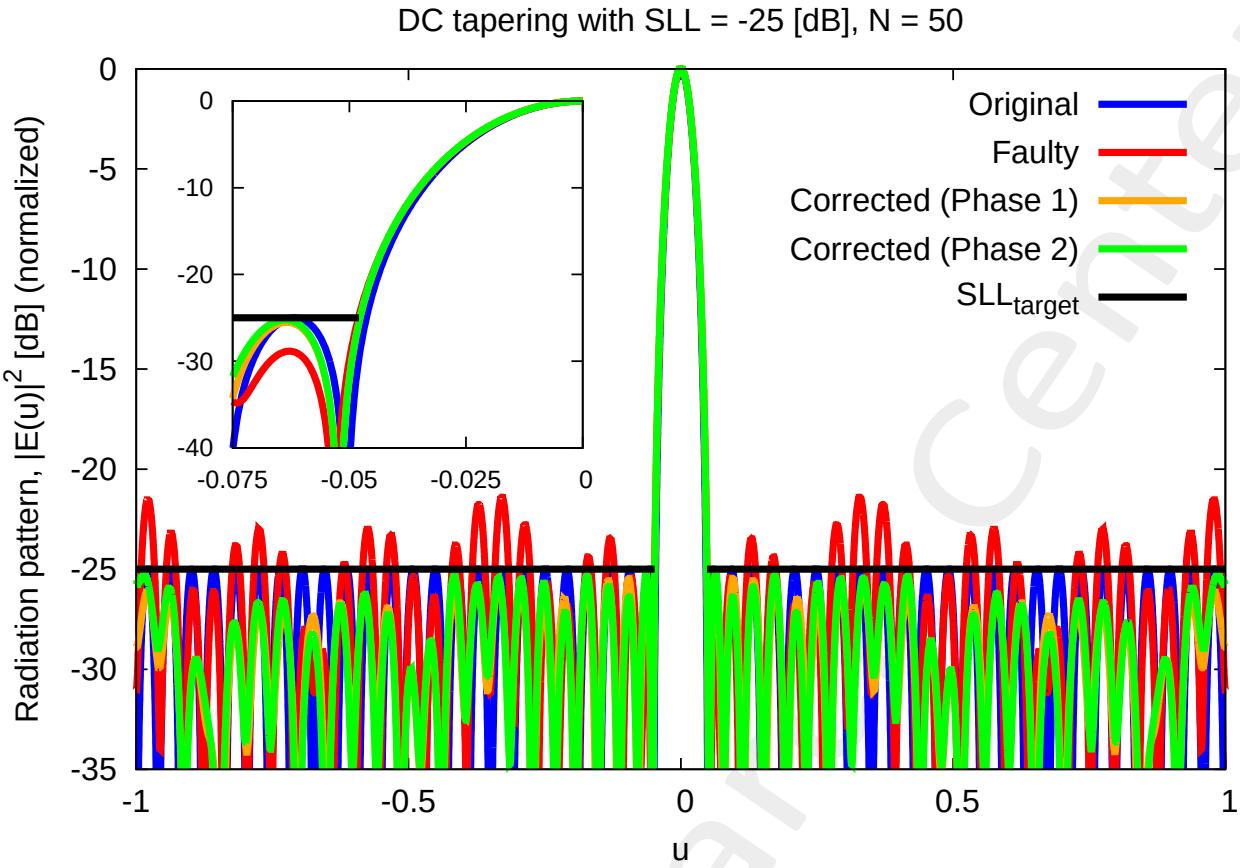

Figure 6: The radiation pattern for the original, faulty and corrected excitations for the array with 50 elements. The smaller rectangle within the figure shows the peak side lobe of the faulty-state pattern being suppressed in the corrected pattern.

Figure 7 shows the value of the L1-norm cost function for each iteration of the algorithm for the array with 50 elements.

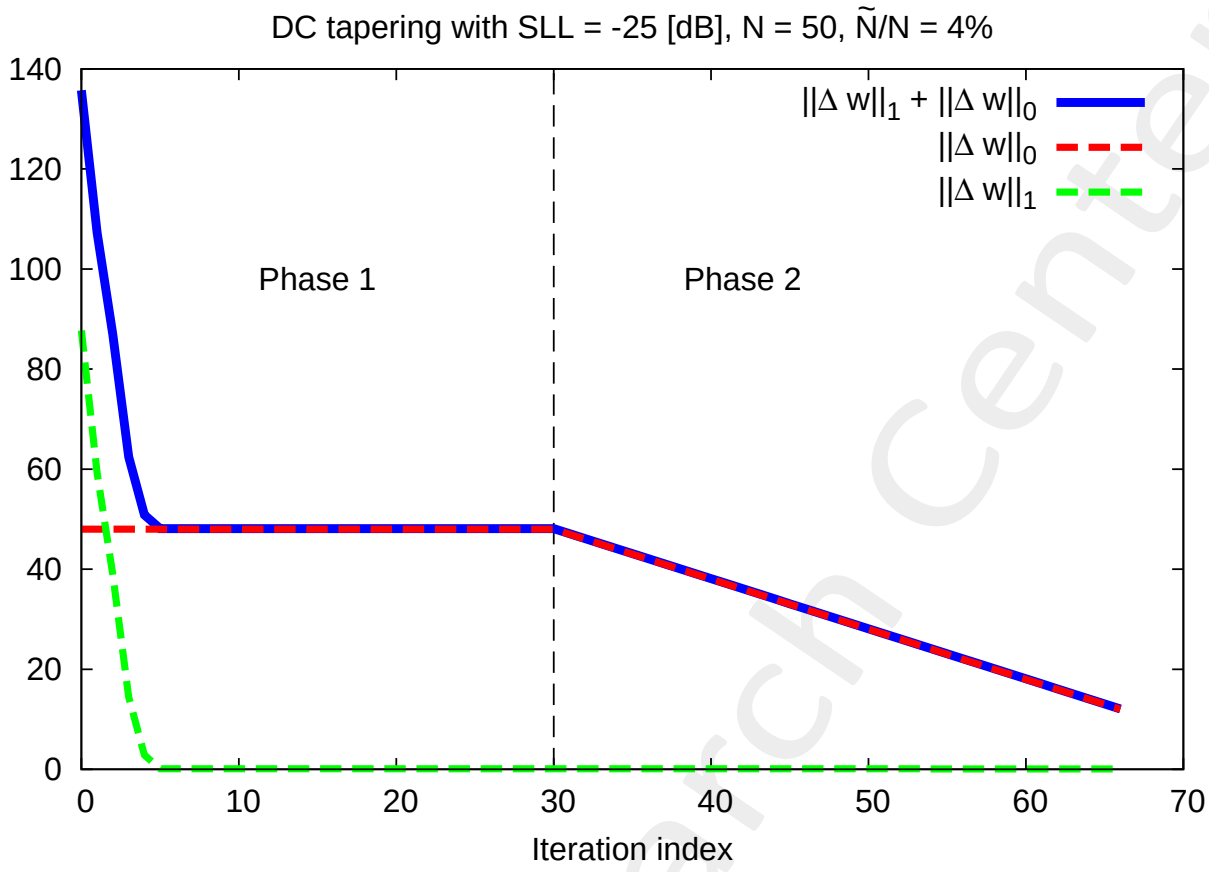

Figure 7: The value of the L1-norm cost function for each iteration of the algorithm for the array with 50 elements.

Table I reports the SLL of the radiation patterns for the original, faulty and corrected excitations for the array with 50 elements.

	Pattern SLL [dB]	HPBW [deg]	DRR	$\left\|\mathbf{w}_{\text{corr,mut}} - \mathbf{w}_{\text{orig,mut}}\right\|_1$	$\left\|\mathbf{w}_{\text{corr,mut}} - \mathbf{w}_{\text{orig,mut}}\right\|_0$
Original excitations	-25.00	2.28	2.59×10^{-1}		
Faulty excitations	-21.41	2.23	2.59×10^{-1}		
Corrected excitations (init.)	-14.35	1.98	1.0×10^{1}	8.30	48
Corrected excitations (Phase 1)	-25.47	2.34	3.94×10^{-1}	3.21	48
Corrected excitations (Phase 2)	-25.22	2.29	3.23×10^{-1}	2.03	12

Table I: Comparison of the original, faulty and corrected excitations.

Array with 100 elements

Figure 8 compares the original excitations with the corrected excitations obtained with the proposed method for the array with 100 elements.

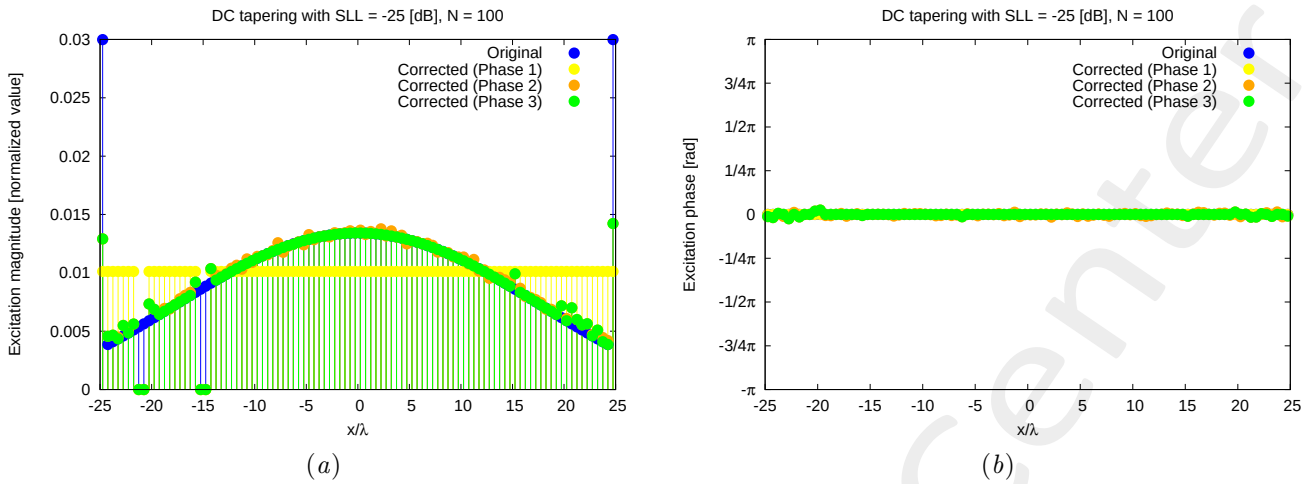

(a) (b)

Figure 8: Original and corrected excitations for the array with 100 elements: amplitude (a) and phase (b).

Figure 9 compares the original, faulty and corrected radiation patterns for the array with 100 elements.

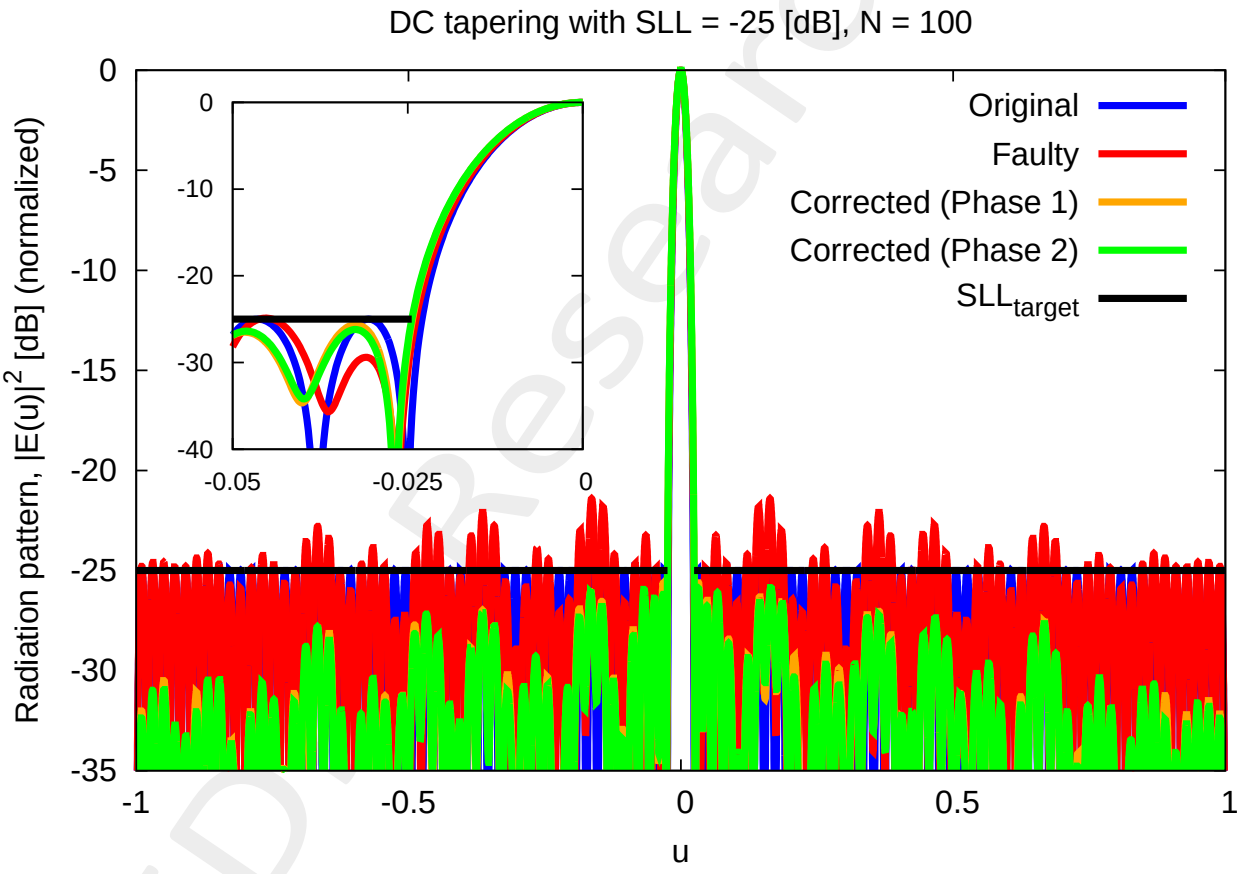

Figure 9: The radiation pattern for the original, faulty and corrected excitations for the array with 100 elements. The smaller rectangle within the figure shows the peak side lobe of the faulty-state pattern being suppressed in the corrected pattern.

Figure 10 shows the value of the L1-norm cost function for each iteration of the algorithm for the array with 100 elements.

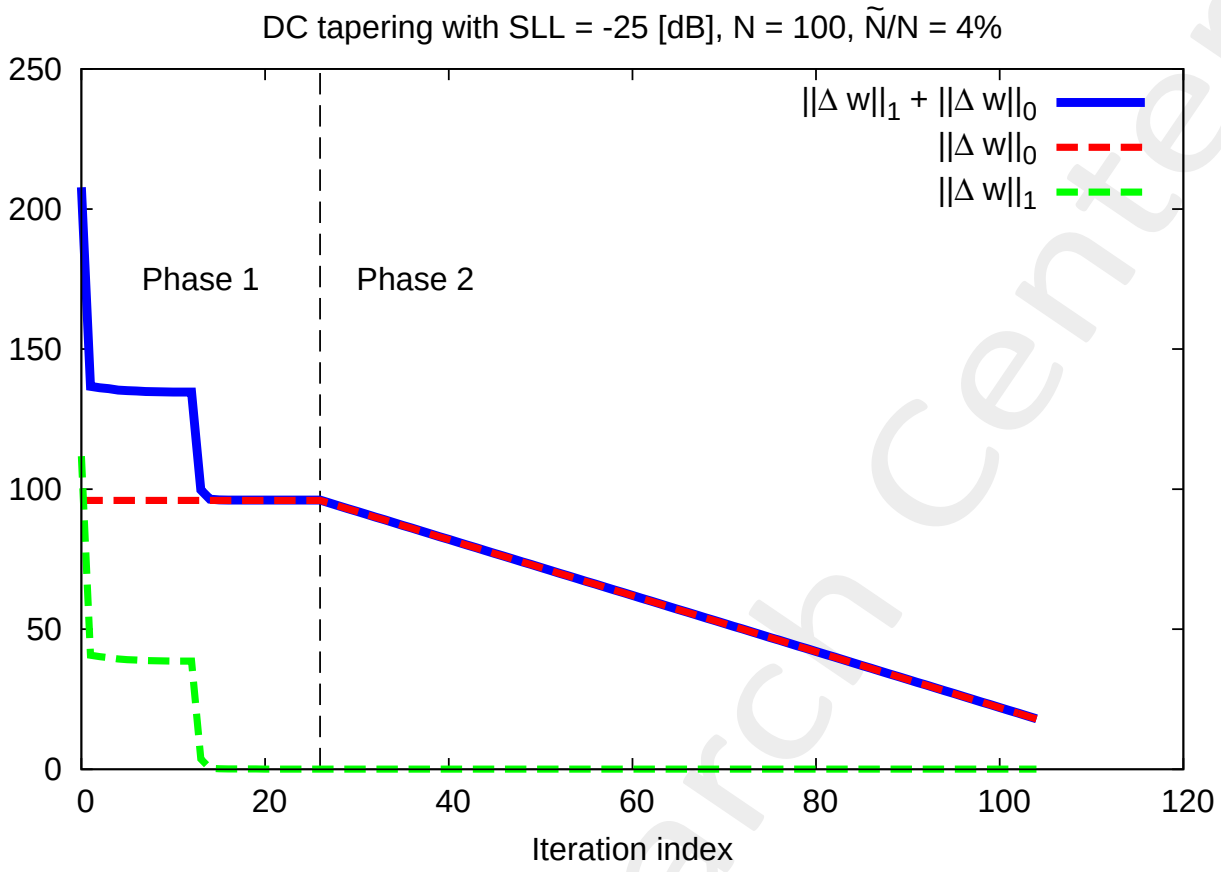

Figure 10: The value of the L1-norm cost function for each iteration of the algorithm for the array with 100 elements.

Table II reports the SLL of the radiation patterns for the original, faulty and corrected excitations for the array with 100 elements.

	Pattern SLL [dB]	HPBW [deg]	DRR	$\left\|\mathbf{w}_{\text{corr,mut}} - \mathbf{w}_{\text{orig,mut}}\right\|_1$	$\left\|\mathbf{w}_{\text{corr,mut}} - \mathbf{w}_{\text{orig,mut}}\right\|_0$
Original excitations	-25.00	1.13	1.29×10^{-1}		
Faulty excitations	-21.42	1.10	1.29×10^{-1}		
Corrected excitations (init.)	-14.38	0.99	1.0	9.66	96
Corrected excitations (Phase 1)	-25.61	1.12	2.95×10^{-1}	2.29	96
Corrected excitations (Phase 2)	-25.86	1.11	2.71×10^{-1}	1.58	18

Table II: Comparison of the original, faulty and corrected excitations.

Array with 150 elements

Figure 11 compares the original excitations with the corrected excitations obtained with the proposed method for the array with 100 elements.

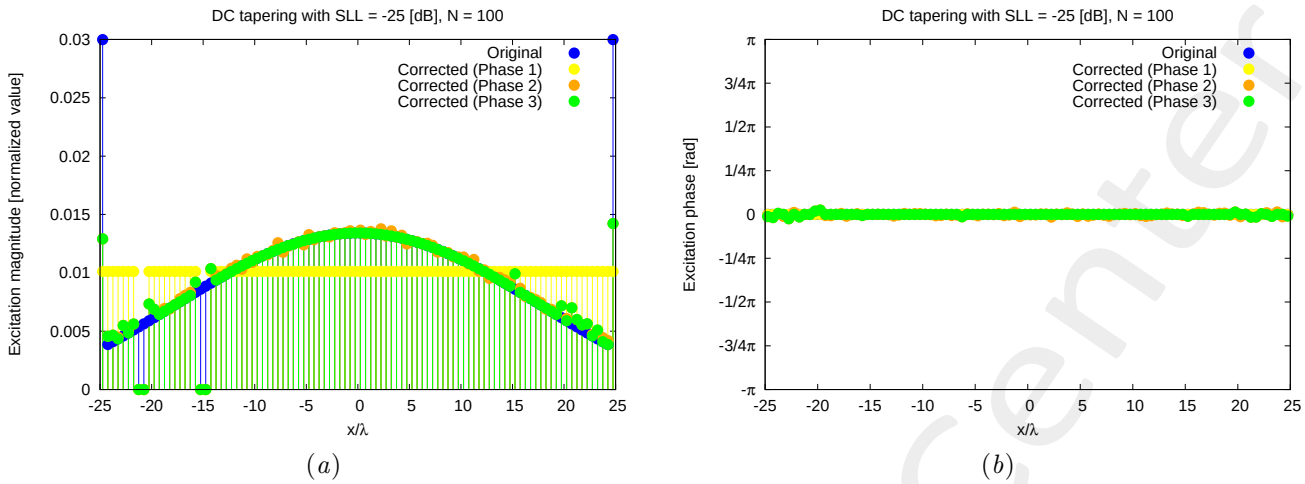

Figure 11: Original and corrected excitations for the array with 150 elements: amplitude (a) and phase (b).

Figure 12 compares the original, faulty and corrected radiation patterns for the array with 150 elements.

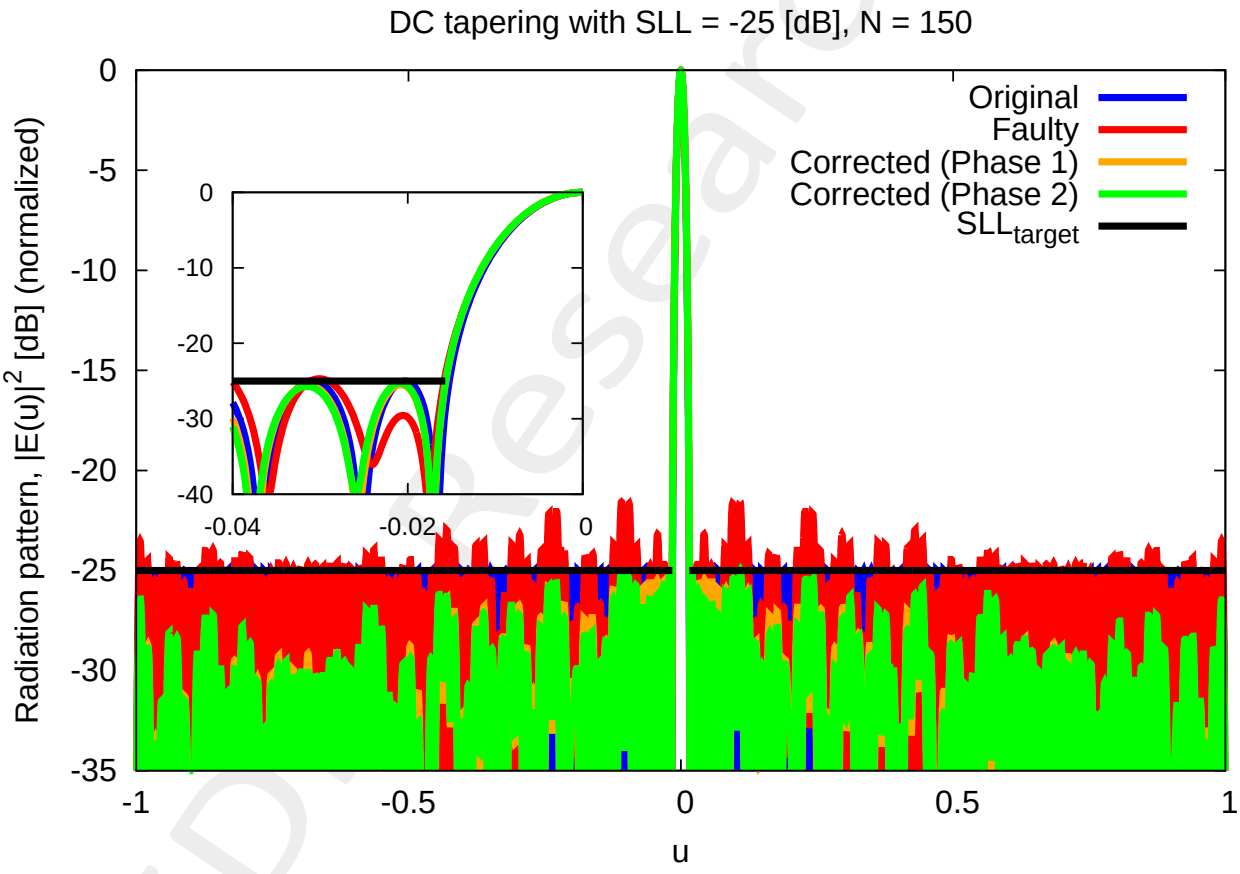

Figure 12: The radiation pattern for the original, faulty and corrected excitations for the array with 150 elements. The smaller rectangle within the figure shows the peak side lobe of the faulty-state pattern being suppressed in the corrected pattern.

Figure 13 shows the value of the L1-norm cost function for each iteration of the algorithm for the array with 150 elements.

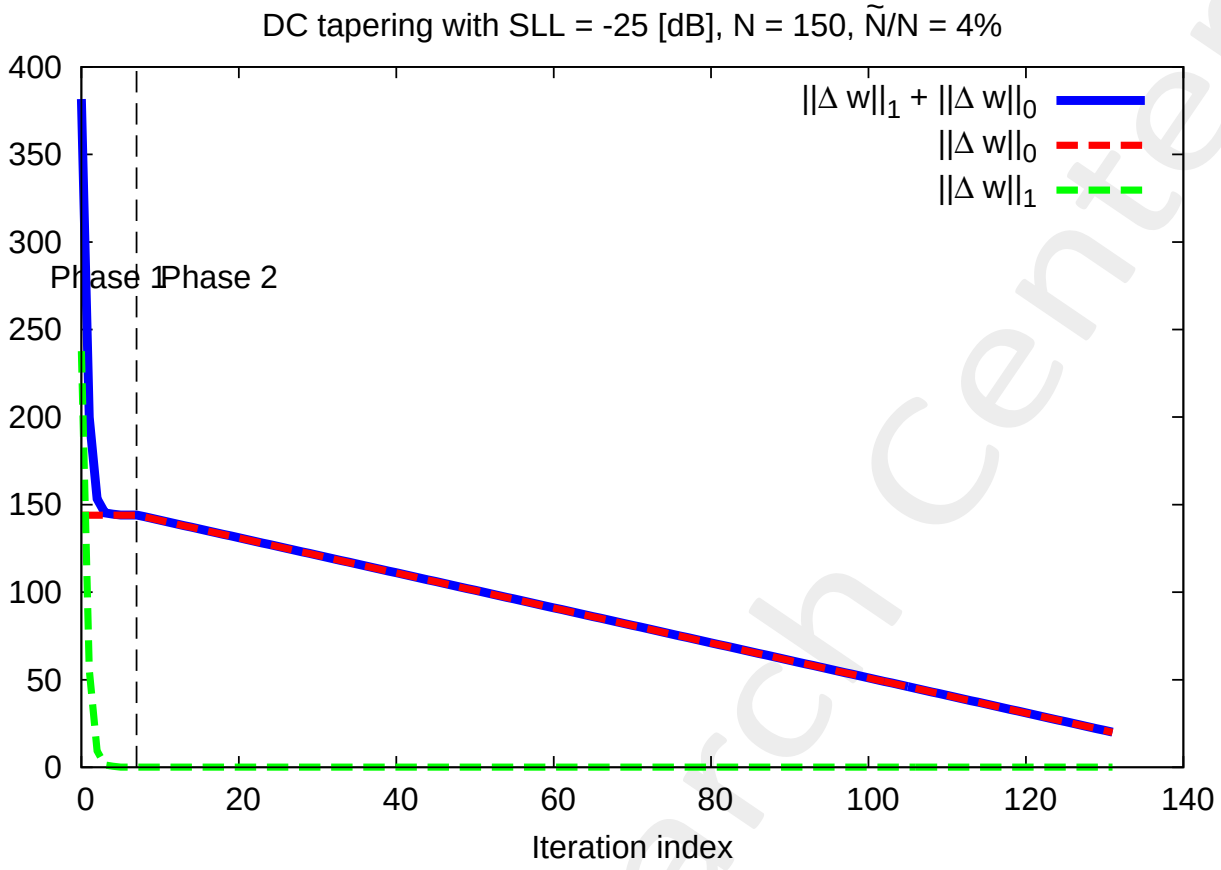

Figure 13: The value of the L1-norm cost function for each iteration of the algorithm for the array with 150 elements.

Table III reports the SLL of the radiation patterns for the original, faulty and corrected excitations for the array with 150 elements.

	Pattern SLL [dB]	HPBW [deg]	DRR	$\left\|\mathbf{w}_{\text{corr,mut}} - \mathbf{w}_{\text{orig,mut}}\right\|_1$	$\left\|\mathbf{w}_{\text{corr,mut}} - \mathbf{w}_{\text{orig,mut}}\right\|_0$
Original excitations	-25.00	0.75	8.55×10^{-2}		
Faulty excitations	-21.58	0.73	8.55×10^{-2}		
Corrected excitations (init.)	-14.39	0.66	1.0	10.2	144
Corrected excitations (Phase 1)	-25.48	0.77	1.76×10^{-1}	3.70	144
Corrected excitations (Phase 2)	-24.99	0.75	1.44×10^{-1}	2.00	20

Table III: Comparison of the original, faulty and corrected excitations.

Array with 200 elements

Figure 14 compares the original excitations with the corrected excitations obtained with the proposed method for the array with 200 elements.

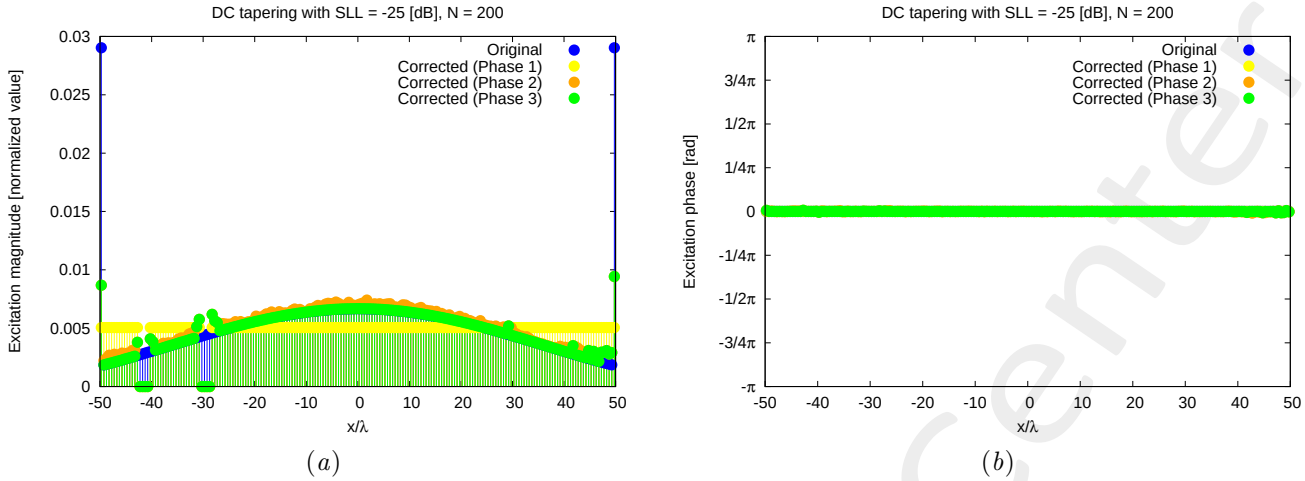

Figure 14: Original and corrected excitations for the array with 200 elements: amplitude (a) and phase (b).

Figure 15 compares the original, faulty and corrected radiation patterns for the array with 200 elements.

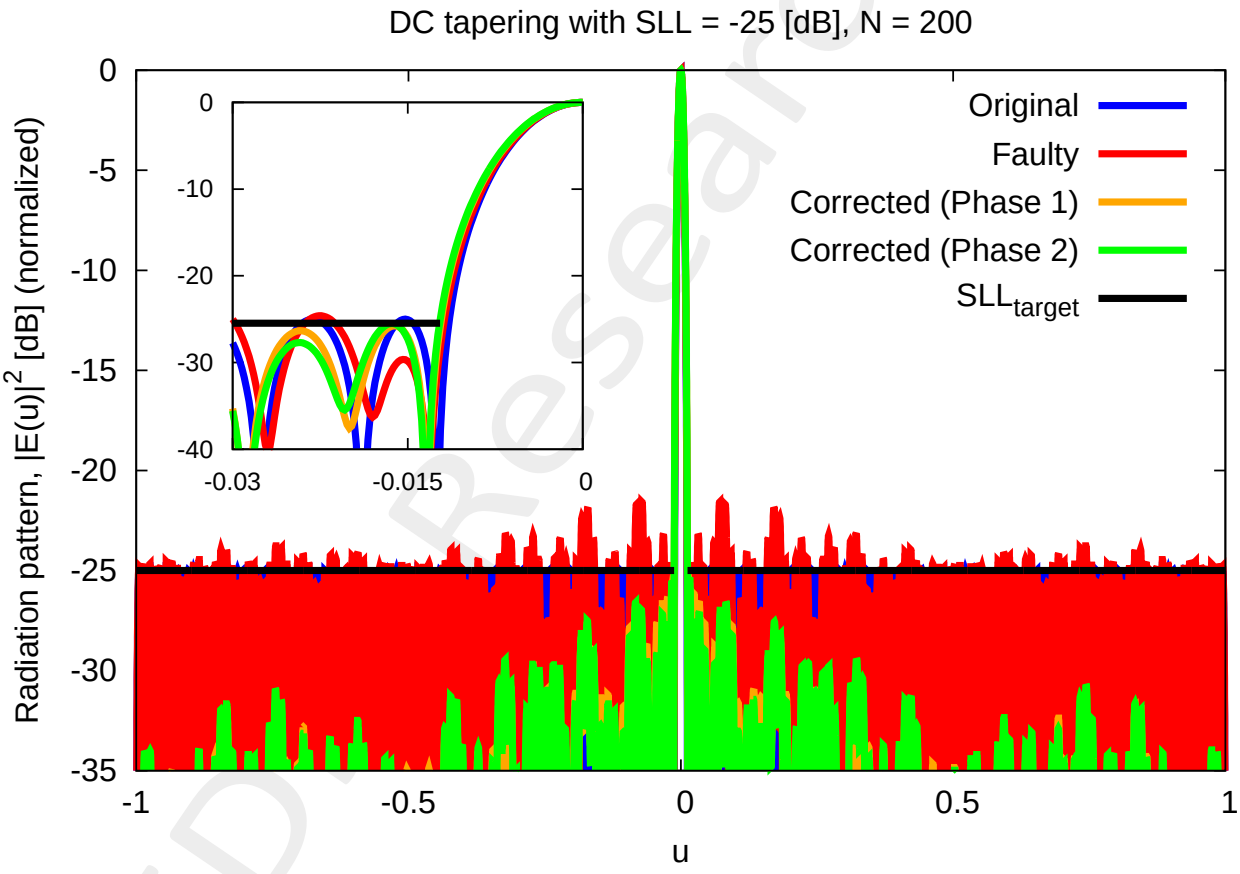

Figure 15: The radiation pattern for the original, faulty and corrected excitations for the array with 200 elements. The smaller rectangle within the figure shows the peak side lobe of the faulty-state pattern being suppressed in the corrected pattern.

Figure 16 shows the value of the L1-norm cost function for each iteration of the algorithm for the array with 200 elements.

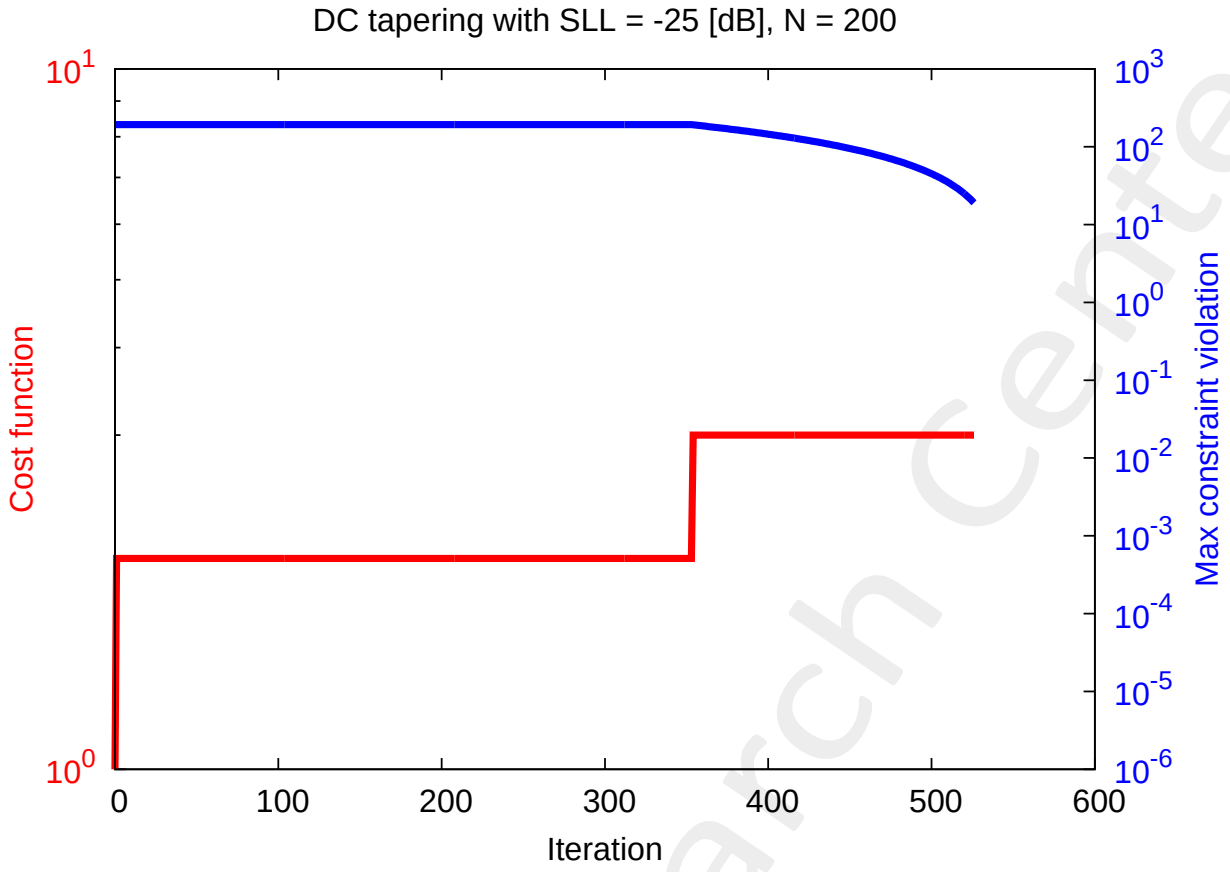

Figure 16: The value of the L1-norm cost function for each iteration of the algorithm for the array with 200 elements.

Table IV reports the SLL of the radiation patterns for the original, faulty and corrected excitations for the array with 200 elements.

	Pattern SLL [dB]	HPBW [deg]	DRR	$\left\|\mathbf{w}_{\text{corr,mut}} - \mathbf{w}_{\text{orig,mut}}\right\|_1$	$\left\|\mathbf{w}_{\text{corr,mut}} - \mathbf{w}_{\text{orig,mut}}\right\|_0$
Original excitations	-25.00	0.56	6.41×10^{-2}		
Faulty excitations	-21.58	0.55	6.41×10^{-2}		
Corrected excitations (init.)	-14.39	0.49	1.0	10.4	192
Corrected excitations (Phase 1)	-25.62	0.59	2.35×10^{-1}	3.90	192
Corrected excitations (Phase 2)	-25.33	0.55	1.97×10^{-1}	1.94	19

Table IV: Comparison of the original, faulty and corrected excitations.

Summary

Table V the number of corrected excitations for the three array dimensions considered in Test case 5.

Total array elements, N	$\|\Delta\mathbf{w}\|_0$	$\|\Delta\mathbf{w}\|_0 / N$
50	12	24%
100	18	18%
150	20	13.3%
200	19	9.5%

Table V: Number of corrected excitations for the three array dimensions considered.

1.1.4 Observations

As seen in Table V, the relative number of elements changed by the algorithm reduces as the array size increases.

More information on the topics of this document can be found in the following list of references.

References

[1] A. Massa, P. Rocca, and G. Oliveri, "Compressive sensing in electromagnetics - A review," *IEEE Antennas Propag. Mag.*, pp. 224-238, vol. 57, no. 1, Feb. 2015.

[2] A. Massa and F. Texeira, "Guest-Editorial: Special Cluster on Compressive Sensing as Applied to Electromagnetics," *IEEE Antennas Wireless Propag. Lett.*, vol. 14, pp. 1022-1026, 2015.

[3] F. Zardi, G. Oliveri, M. Salucci, and A. Massa, "Minimum-complexity failure correction in linear arrays via compressive processing," *IEEE Trans. Antennas Propag.*, vol. 69, no. 8, pp. 4504-4516, Aug. 2021.

[4] N. Anselmi, G. Gottardi, G. Oliveri, and A. Massa, "A total-variation sparseness-promoting method for the synthesis of contiguously clustered linear architectures" *IEEE Trans. Antennas Propag.*, vol. 67, no. 7, pp. 4589-4601, Jul. 2019.

[5] M. Salucci, A. Gelmini, G. Oliveri, and A. Massa, "Planar arrays diagnosis by means of an advanced Bayesian compressive processing," *IEEE Tran. Antennas Propag.*, vol. 66, no. 11, pp. 5892-5906, Nov. 2018.

[6] L. Poli, G. Oliveri, P. Rocca, M. Salucci, and A. Massa, "Long-Distance WPT Unconventional Arrays Synthesis" *Journal of Electromagnetic Waves and Applications*, vol. 31, no. 14, pp. 1399-1420, Jul. 2017.

[7] G. Oliveri, M. Salucci, and A. Massa, "Synthesis of modular contiguously clustered linear arrays through a sparseness-regularized solver," *IEEE Trans. Antennas Propag.*, vol. 64, no. 10, pp. 4277-4287, Oct. 2016.

[8] M. Carlin, G. Oliveri, and A. Massa, "Hybrid BCS-deterministic approach for sparse concentric ring isophoric arrays," *IEEE Trans. Antennas Propag.*, vol. 63, no. 1, pp. 378-383, Jan. 2015.

[9] G. Oliveri, E. T. Bekele, F. Robol, and A. Massa, "Sparsening conformal arrays through a versatile BCS-based method," *IEEE Trans. Antennas Propag.*, vol. 62, no. 4, pp. 1681-1689, Apr. 2014.

[10] F. Viani, G. Oliveri, and A. Massa, "Compressive sensing pattern matching techniques for synthesizing planar sparse arrays," *IEEE Trans. Antennas Propag.*, vol. 61, no. 9, pp. 4577-4587, Sept. 2013.

[11] G. Oliveri, P. Rocca, and A. Massa, "Reliable diagnosis of large linear arrays - A Bayesian Compressive Sensing approach," *IEEE Trans. Antennas Propag.*, vol. 60, no. 10, pp. 4627-4636, Oct. 2012.

[12] G. Oliveri, M. Carlin, and A. Massa, "Complex-weight sparse linear array synthesis by Bayesian Compressive Sampling," *IEEE Trans. Antennas Propag.*, vol. 60, no. 5, pp. 2309-2326, May 2012.

[13] G. Oliveri and A. Massa, "Bayesian compressive sampling for pattern synthesis with maximally sparse non-uniform linear arrays," *IEEE Trans. Antennas Propag.*, vol. 59, no. 2, pp. 467-481, Feb. 2011.

[14] P. Rocca, M. A. Hannan, M. Salucci, and A. Massa, "Single-snapshot DoA estimation in array antennas with mutual coupling through a multi-scaling BCS strategy," *IEEE Trans. Antennas Propag.*, vol. 65, no. 6, pp. 3203-3213, Jun. 2017.

[15] B. Li, M. Salucci, W. Tang, and P. Rocca, "Reliable field strength prediction through an adaptive total-variation CS technique," *IEEE Antennas Wireless Propag. Lett.*, vol. 19, no. 9, pp. 1566-1570, Sep. 2020.

[16] M. Salucci, M. D. Migliore, P. Rocca, A. Polo, and A. Massa, "Reliable antenna measurements in a near-field cylindrical setup with a sparsity promoting approach," *IEEE Trans. Antennas Propag.*, vol. 68, no. 5, pp. 4143-4148, May 2020.

[17] A. Benoni, P. Rocca, N. Anselmi, and A. Massa, "Hilbert-ordering based clustering of complex-excitations linear arrays," *IEEE Trans. Antennas Propag.*, vol. 70, no. 8, pp. 6751-6762, Aug. 2022.

[18] P. Rocca, L. Poli, N. Anselmi, and A. Massa, "Nested optimization for the synthesis of asymmetric shaped beam patterns in sub-arrayed linear antenna arrays," *IEEE Trans. Antennas Propag.*, vol. 70, no. 5, pp. 3385 - 3397, May 2022.

[19] P. Rocca, L. Poli, A. Polo, and A. Massa, "Optimal excitation matching strategy for sub-arrayed phased linear arrays generating arbitrary shaped beams," *IEEE Trans. Antennas Propag.*, vol. 68, no. 6, pp. 4638-4647, Jun. 2020.

[20] G. Oliveri, G. Gottardi and A. Massa, "A new meta-paradigm for the synthesis of antenna arrays for future wireless communications," *IEEE Trans. Antennas Propag.*, vol. 67, no. 6, pp. 3774-3788, Jun. 2019.

[21] P. Rocca, M. H. Hannan, L. Poli, N. Anselmi, and A. Massa, "Optimal phase-matching strategy for beam scanning of sub-arrayed phased arrays," *IEEE Trans. Antennas Propag.*, vol. 67, no. 2, pp. 951-959, Feb. 2019.

[22] N. Anselmi, P. Rocca, M. Salucci, and A. Massa, "Contiguous phase-clustering in multibeam-on-receive scanning arrays" *IEEE Trans. Antennas Propag.*, vol. 66, no. 11, pp. 5879-5891, Nov. 2018.

[23] G. Gottardi, L. Poli, P. Rocca, A. Montanari, A. Aprile, and A. Massa, "Optimal Monopulse Beamforming for Side-Looking Airborne Radars," *IEEE Antennas Wireless Propag. Lett.*, vol. 16, pp. 1221-1224, 2017.

[24] P. Rocca, G. Oliveri, R. J. Mailloux, and A. Massa, "Unconventional phased array architectures and design Methodologies - A review" *Proceedings of the IEEE - Special Issue on 'Phased Array Technologies*', Invited Paper, vol. 104, no. 3, pp. 544-560, March 2016.

[25] P. Rocca, M. D'Urso, and L. Poli, "Advanced strategy for large antenna array design with subarray-only amplitude and phase control," *IEEE Antennas and Wireless Propag. Lett.*, vol. 13, pp. 91-94, 2014.

[26] L. Manica, P. Rocca, G. Oliveri, and A. Massa, "Synthesis of multi-beam sub-arrayed antennas through an excitation matching strategy," *IEEE Trans. Antennas Propag.*, vol. 59, no. 2, pp. 482-492, Feb. 2011.

[27] M. Salucci, G. Oliveri, and A. Massa, "An innovative inverse source approach for the feasibility-driven design of reflectarrays," *IEEE Trans. Antennas Propag.*, vol. 70, no. 7, pp. 5468-5480, July 2022.

[28] L. T. P. Bui, N. Anselmi, T. Isernia, P. Rocca, and A. F. Morabito, "On bandwidth maximization of fixed-geometry arrays through convex programming," *Journal of Electromagnetic Waves and Applications*, vol. 34, no. 5, pp. 581-600, 2020.

[29] N. Anselmi, L. Poli, P. Rocca, and A. Massa, "Design of simplified array layouts for preliminary experimental testing and validation of large AESAs," *IEEE Trans. Antennas Propag.*, vol. 66, no. 12, pp. 6906-6920, Dec. 2018.

[30] G. Gottardi, L. Poli, P. Rocca, A. Montanari, A. Aprile, and A. Massa, "Optimal Monopulse Beamforming for Side-Looking Airborne Radars," *IEEE Antennas Wireless Propag. Lett.*, vol. 16, pp. 1221-1224, 2017.

[31] G. Oliveri and T. Moriyama, "Hybrid PS-CP technique for the synthesis of n-uniform linear arrays with maximum directivi" *Journal of Electromagnetic Waves and Applications*, vol. 29, no. 1, pp. 113-123, Jan. 2015.

[32] P. Rocca and A. Morabito, "Optimal synthesis of reconfigurable planar arrays with simplified architectures for monopulse radar applications" *IEEE Trans. Antennas Propag.*, vol. 63, no. 3, pp. 1048-1058, Mar. 2015.

[33] A. F. Morabito and P. Rocca, "Reducing the number of elements in phase-only reconfigurable arrays generating sum and difference patterns," *IEEE Antennas Wireless Propag. Lett.*, vol. 14, pp. 1338-1341, 2015.

[34] P. Rocca, N. Anselmi, and A. Massa, "Optimal synthesis of robust beamformer weights exploiting interval analysis and convex optimization," *IEEE Trans. Antennas Propag.*, vol. 62, no. 7, pp. 3603-3612, Jul. 2014.